Journal of Drug Targeting, 2011, 19(4): 303–313
© 2011 Informa UK, Ltd.
ISSN 1061-186X print/ISSN 1029-2330 online
DOI: 10.3109/1061186X.2010.499466

informa
healthcare

ORIGINAL ARTICLE

pH-sensitive PEG-based micelles for tumor targeting

Stefano Salmaso, Sara Bersani, Marco Pirazzini, and Paolo Caliceti

Department of Pharmaceutical Sciences, University of Padova, Padova, Italy

Abstract

A new acid sensitive nanocarrier based on lipid core micelles has been investigated for tumor targeted drug delivery. Sulfadimethoxine-PEG-phospholipid unimer (SD-PEG-DSPE) was designed to endow micelles with pH responsiveness in the physiopathologic range. The unimer was synthesized according to a two-step procedure. Potentiometric analysis showed that SD-PEG-DSPE has pK_a of 6.7. In water, the unimers assembled spontaneously in 20 nm size micelles with 60 μM critical micelle concentration. The particle size was not affected by the pH in the 6.2–7.4 range. The micelles loaded paclitaxel very efficiently and released the drug slowly regardless the incubation pH. Fluorescence spectroscopy and cytofluorimetry carried out by MCF7 tumor cell incubation with labeled SD-PEG-DSPE micelles at pH 7.4 and 6.2 showed that micelles associate with cells mostly at acidic pH with a time-dependent behavior. A cell subpopulation took up the nanocarrier more efficiently at pH 6.2. Confocal microscopy confirmed that under these conditions the systems are taken up by cells or fuse with cellular membrane. Cytotoxicity studies demonstrated that the SD-PEG-DSPE micelles deliver more efficiently paclitaxel at pH 6.2 than at neutral pH confirming that the cell internalization can be triggered by the external environmental conditions.

Keywords: pH-sensitive micelles, paclitaxel, nanocarrier, PEG-phospholipid colloidal systems

Journal of Drug Targeting Downloaded from informahealthcare.com by Radboud Universiteit Nijmegen on 11/04/14
For personal use only.

Introduction

In the last decades, nanoscience has been playing a pivotal role in the investigation of novel biophysical phenomena, processes, and materials at the nanometer scale that find application in many fields of life and health science. Nanotechnology advancements have provided for a wide range of tools and devices with unique features that can be properly exploited in therapeutic, diagnostic, and regenerative science. Accordingly, physical or chemical combination of molecular modules with different physicochemical and biological properties may afford nanocarriers with complex architectures and "smart" behavior. Surface tailoring, for example, can yield selective biological recognition and drug targeting to specific tissues and avoid unwanted nanosystem interface interactions with biological structures, namely cells and proteins.

So far, a variety of nanospheres have been investigated and exploited for controlled release of drugs with poor biopharmaceutical properties (Panyam & Labhasetwar, 2003; Salmaso et al., 2009; Kumari et al., 2010). Nevertheless, inadequate size, shape, and surface properties often represent a hurdle to their systemic administration and circulation in the blood stream. Poor physicochemical features may provoke aggregation, microvessel clogging and promote opsonization followed by complement activation and removal by the RES (De & Robinson, 2004; Makino et al. 2001). These drawbacks hamper their biopharmaceutical efficiency, application reliability, and safety, which exclude their use as circulating carriers for site-specific drug delivery (Verrecchia et al., 1995; Owens 3rd & Peppas, 2006).

Amphiphilic materials that self assemble into colloidal hydrophobic core/hydrophilic shell particles have been successfully developed as drug carriers as they can host poorly soluble and unstable drugs into the core while drug release occurs by physical mechanism which involve drug diffusion or particle disaggregation. According to their physicochemical properties, these systems can display long circulating properties and disease site tropism thus enhancing the body exposure to the drug. As an example, lipid core PEG nanocarriers with diameter up to 300 nm have been investigated for tumor targeting as they can accumulate into the tumor

Address for Correspondence: Stefano Salmaso, Department of Pharmaceutical Sciences, University of Padova, Via F. Marzolo 5, 35131 Padova, Italy. E-mail: stefano.salmaso@unipd.it

(Received 22 March 2010; revised 22 May 2010; accepted 24 May 2010)

RIGHTSLINK

tissue by the enhanced permeability and retention effect (Matsumura & Maeda, 1986; Yokoyama et al., 1990; Lukyanov & Torchilin, 2004; Torchilin, 2007). Nevertheless, due to the lack of cell recognition properties, plain micelles can distribute into the disease site only by passive mechanisms that strongly limit the selectivity of these formulations. Aimed at improving the therapeutic performance of nanosystems, many efforts have been dedicated to prepare smart carriers with cell recognition moieties or environmentally sensitive modules that can target selectively tissues and cells, as well as interact with them, undergo cell uptake, and release the drug into specific compartments by physiopathological stimuli. Based on evidences that cancer tissues have altered biological activity that affects temperature, pH, enzyme composition, and redox activity, stimuli sensitive colloidal drug delivery systems that exploit the healthy tissue/disease tissue microenvironmental differences have been designed for anticancer drug delivery (Tannock & Rotin, 1989; Gerweck & Seetharaman, 1996; Stefanadis et al., 2001). pH-sensitive nanoparticles have interesting perspectives as anticancer drug delivery systems as they undergo increased cell association under slightly acidic conditions, which mimic the tumor interstitial conditions (Na et al., 2003). However, since the pH environmental differences are very sharp, nanosystems provided with adequate "molecular sensors" having very precise responsiveness within narrow environmental differences are required. A screening of molecular sensors with pH sensitiveness that guarantee for hydrophilic/hydrophobic switching suitable for controlled drug release was first published by Bae and co-workers (Kang & Bae, 2001, 2002). Sulfadimethoxine (SD) has been associated to hardcore matrix–based or hydrogels core–based nanoparticles to produce pH responsive formulations. According to its pK_a of 6.2, SD can in fact undergo reversible pH-dependent protonation that induces structural hydrophilic/hydrophobic changes. Therefore, the drug release rate from these nanosystems is governed mostly by pH controlled core shrinking (Na et al., 2004).

Although phospholipids-PEG pH responsive micelles offer new interesting opportunities to the anticancer drug delivery, there is still a lack of investigation about the physicochemical requisites that dictate the biopharmaceutical behavior and benefits of these systems. In order to advance the knowledge on the key parameters that affect the drug delivery properties of pH-sensitive colloidal systems, new phospholipid-PEG micelles decorated with multiple copies of a pH responsive moiety have been produced. The pH-sensitive molecule was selected to modulate the surface properties of the nanocarrier (namely hydrophilic/hydrophobic features) according to narrow pH changes throughout the body districts. *In vitro* studies were carried out using paclitaxel as anticancer drug model to examine the physicochemical and biopharmaceutical properties of these systems and their effective potential as drug delivery systems.

Materials and methods

Materials

1,2-Distearoyl-*sn*-glycero-3-phosphoethanolamine-N-[*N*-Hydroxysuccinimidyl (poly(ethylene glycol))-3400] (NHS-$PEG_{3.4\ kDa}$-DSPE) and 1,2-distearoyl-*sn*-glycero-3-phosphoethanolamine-*N*-[methoxy (poly(ethylene glycol))5000] ($mPEG_{5\ kDa}$-DSPE) were purchased from Laysan Bio Inc. (Arab, AL). Paclitaxel was from LC Laboratories (Woburn, MA). 1,2-Dioleoyl-*sn*-glycero-3-phosphoethanolamine-fluorescein (fluorescein-DOPE), pyrene, MTT, cell culture media, penicillin-streptomicin-amphotericin B solution, trypsin solution, fetal bovine serum (FBS) were obtained from Sigma (St. Louis, MO). SD, succinic anhydride and 1,2-diaminoethane (DAE) were purchased from Fluka (Buchs, Switzerland). All analytical grade and deuterated solvents were obtained from Aldrich (Ostheim, Germany).

Sephadex G 25 superfine medium was provided by GE Healthcare Bio-sciences AB (Uppsala, Sweden). Human breast adenocarcinoma MCF7 cells were cultured in RPMI-1640 medium supplemented with 10% fetal calf serum, 2 mM glutamine, 100 IU/mL penicillin, 100 μg/mL streptomycin, 0.25 μg/mL amphotericin B. Cells were routinely treated with a 500 μg/mL trypsin solution containing 2.5 mg/mL EDTA in Ca^{2+} and Mg^{2+} free 0.02 M phosphate buffer, 0.15 M NaCl, pH 7.4 and transferred on a new flask.

Synthesis of SD-succinate

SD (2.0 g, 6.4 mmol) was dissolved in 45 mL of anhydrous acetone. The solution was added of succinic anhydride (3.2 g, 32 mmol) and stirred overnight under anhydrous conditions. The white precipitate was recovered by centrifugation and washed three times with acetone. The product was dried under vacuum and recovered at 62.6% yield. Thin-layer chromatography of the product was carried out on glass sheets coated with silica gel (Merck F-254; Merck, Darmstadt, Germany). The plates were run with $CHCl_3$/methanol 12/1 volume ratio and detected by 254 nm UV light. SD-succinate (SD-succ) and SD showed R_f of 0.85 and 0.89, respectively. The purity of the intermediate was evaluated by RP-HPLC using a Shimadzu SP-10 HPLC system equipped with a Phenomenex Luna C_{18} column (250 × 4.6 mm) eluted in a gradient mode, using water-0.05% trifluoroacetic acid (TFA) (eluent A) and acetonitrile-0.05% TFA (eluent B), from 15% to 50% eluent B in 17 min. The UV detector was set at 268 nm. SD-succ was found to have 98% purity. The product was analyzed by ^{1}H NMR spectroscopy using a Bruker Spectrospin 300, 300 MHz (Bruker Spectrospin, Billerica, MA).

^{1}H NMR in DMSO-d6: δ 2.60 (t, J = 6.2 Hz, 2 H of succinic acid -NH-CO-CH_2-CH_2-); δ 2.67 (t, J = 6.3 Hz, 2 H of succinic acid NH-CO-CH_2-CH_2-); δ 3.35 (s, 1 H of aromatic anilinamide -N*H*-COO-CH_2-); δ 3.75 and 3.79 (ds, 6 H, -OCH_3 of pyrimidinic ring); δ 5.93 (s, 1 H, pyrimidinic ring); δ 7.88 (d, J = 9.2 Hz, 2 H, protons of aromatic

Journal of Drug Targeting Downloaded from informahealthcare.com by Radboud Universiteit Nijmegen on 11/04/14
For personal use only.

RIGHTSLINK

anilinamide ring); δ 7.74 (d, J= 9.2, 2 H, protons of aromatic anilinamide ring); δ 10.40 (s, 1 H of -N*H*SO_2-).

The final product (SD-succ) dissolved in methanol (1 mg/mL) was analyzed by mass spectroscopy using a Mariner ESI-TOF system (PerSeptive Biosystems, Framingham, MA). The positive ion was found to have 411.10 *m/z* [calculated for $(M+H)^+$: 411.09].

Synthesis of SD-succ methyl ester (SD-succ-OCH_3)

SD-succ (400 mg, 973 μmol) was dissolved in 25 mL of methanol in presence of 500 μL of acetyl chloride (9.7 mmol). After 30-min reaction, $NaHCO_3$ (706 mg, 8.40 mmol) was added to quench the hydrogen chloride released by the esterification reaction. The methanolic solution was evaporated under reduced pressure. A total recovery of the product was achieved.

^1H NMR in DMSO-d6: δ 2.60 (t, J = 6.2 Hz, 2 H of succinic acid NH-CO-CH_2-C*H*$_2$-); δ 2.67 (t, J = 6.3 Hz, 2 H of succinic acid NH-CO-C*H*$_2$-CH_2-); δ 3.35 (s, 1 H of aromatic anilinamide -N*H*-COO-CH_2-); δ 3.58 (s, 3 H, -CO-OC*H*$_3$); δ 3.75 and 3.79 (ds, 6 H, -OC*H*$_3$ of pyrimidinic ring); δ 5.93 (s, 1 H, pyrimidinic ring); δ 7.88 (d, J = 9.2, 2 H, protons of aromatic anilinamide ring); δ 7.74 (d, J = 9.2, 2H, protons of aromatic anilinamide ring); δ 10.40 (s, 1 H of -N*H*SO_2-).

The chemical identity of the SD-succ-OCH_3 was confirmed by ESI-TOF mass spectrometry that showed *m/z* signal of 425.14 [calculated for $(M+H^+)$: 425.12]. The purity of the intermediate was evaluated by RP-HPLC as reported above and was found to be 95.5%.

Synthesis of SD-succ-$CONH(CH_2)_2NH_2$ (SD-succ-ethyl-NH_2)

SD-succ-OCH_3 (413 mg, 971 μmol) was dissolved in 12 mL of dimethyl formamide and the solution was added of 1.31 mL of DAE (19.6 mmol) and 0.15 mL of acetic acid (973 μmol). The reaction was stirred for 6 h at 37°C under anhydrous conditions. The mixture was poured dropwise into cold anhydrous diethyl ether under stirring and the precipitate was washed three times with diethyl ether and desiccated under vacuum. The white powder was dissolved in 10 mL of water and purified by solid phase extraction with a SEP-PAK C_{18} cartridge from Millipore (Milford, MA) eluted with 20 mL of water to remove unreacted 1,4-diaminoethane and then washed extensively with methanol. The organic solvent was removed under vacuum giving a final product yield of 120 mg (27.3%). The derivative was analyzed by thin-layer chromatography carried out on glass sheets coated with silica gel run by methanol. The products were detected with 254 nm UV light (SD-succ R_f = 0.85; SD-succ-ethyl-NH_2 R_f = 0.29). The purity of SD-succ-ethyl-NH_2, assessed by RP-HPLC as described above, was 84%.

^1H NMR in DMSO-d6: δ 2.42 (t, J = 6.8, 2 H of succinic acid -CH_2-C*H*$_2$-); δ 2.59 (t, J = 6.9, 2 H of succinic acid -C*H*$_2$-CH_2-); δ 2.84 (t, J = 6.3, 2 H, diaminoethane -CH_2-C*H*$_2$-NH_2); δ 3.27 (m, J = 6.2 Hz, 2 H, diaminoethane -C*H*$_2$-CH_2-NH_2); δ 3.62 and δ 3.65 (ds, 6 H, -OC*H*$_3$ of pyrimidinic ring); δ 5.59 (s, 1 H, pyrimidinic ring); δ 7.66 (d, J = 8.6 Hz, 2H, protons of anilinamide ring); δ 7.58 (d, J = 8.8 Hz, 2 H, protons of anilinamide ring); δ 8.08 (t, J= 5.5, 1 H, NH_2-CH_2CH_2-N*H*CO-); δ 10.16 (s, 1 H, -N*H*SO_2-).

ESI-TOF mass spectroscopy showed *m/z* signal at 453.16 and at 227.09 *m/z* corresponding to the mono and double charged ions, respectively [calculated for $(M+H)^+$: 453.16; calculated for $(M+2H)^{2+}$: 227.08].

Synthesis of sulfadimetoxine-PEG-DSPE (SD-PEG-DSPE)

SD-succ-ethyl-NH_2 (125 mg, 277 μmol) was dissolved in 3 mL of anhydrous DMF and added of 38 μL of triethylamine (279 μmol) and 200 mg of commercial NHS-$PEG_{3.4\,kDa}$-DSPE (46.1 μmol). The mixture was maintained overnight under stirring and then the crude was recovered by precipitation in cold anhydrous diethylether. The precipitate was dissolved in 2 mL of dichloromethane, centrifuged at 5000 rpm for 5 min and the organic solvent was removed under vacuum. The dry film was rehydrated by adding 5 mL of 5 mM NH_4Cl, pH 8.0, and the conjugate was purified by size exclusion chromatography with a column prepacked with Sephadex G 25 superfine resin eluted with 5 mM NH_4Cl, pH 8.0. Fractions positive to both UV-Vis analysis at 268 nm and Iodine test (Sims & Snape, 1980) were pooled together and lyophilized. The recovery yield was 62%.

The PEG/SD molar ratio in the conjugate was assessed by quantitative Iodine test for PEG and UV spectroscopic analysis for SD (Sadagopa Ramanujam et al., 1980). The SD/PEG molar ratio was found to be 0.79/1. The conjugate purity was estimated by RP-HPLC that confirmed that no traces of SD-succ-ethyl-NH_2 were detectable. The conjugate purity was 93%.

^1H NMR in $CDCl_3$: δ 0.87 (m, 10 H, -C*H*$_2$-C*H*$_3$ of phospholipid alkyl chains); δ 1.25 (m, ~52 H -$(CH_2)_n$- of phospholipid alkyl chains); δ 1.58 (m, 4 H, -$COOCH_2$-C*H*$_2$- of phospholipid alkyl chains); δ 2.26–3.31 (m, 4 H, -COOC*H*$_2$-CH_2 of phospholipid alkyl chains); δ 3.64 (s, 309 H, -OC*H*$_2$C*H*$_2$O- of PEG); δ 3.86 and 3.89 (ds, 4.6 H, -OC*H*$_3$ of pyrimidinic ring of SD); δ 7.88 (d, J = 8.6 Hz, 2 H, protons of anilinamide ring); δ 7.80 (d, J = 8.6 Hz, 2 H, protons of anilinamide ring).

pK_a assessment of SD-PEG-DSPE

SD-PEG-DSPE (100.0 mg, 23.1 μmol) was dissolved in 20 mL of HCl 0.15 M. The potentiometric analysis was carried out by stepwise addition of 0.15 M NaOH to the SD-PEG-DSPE solution using a radiometer ABU93 Triburette titrator (Radiometer Analytical, Villeurbanne Cedex, France) equipped with three automatic regulated burettes, a double internal voltmeter, and a temperature controller.

Micelles preparation

Micelles were prepared by film rehydration as reported by Zhang and co-workers (2003). SD-PEG-DSPE (10 mg) was dissolved in 10 mL of chloroform. The organic solution was removed under vacuum by rotary evaporation.

Journal of Drug Targeting Downloaded from informahealthcare.com by Radboud Universiteit Nijmegen on 11/04/14
For personal use only.

© 2011 Informa UK, Ltd.

RIGHTSLINK

The dry thin layer was rehydrated with 5 mL of 0.02 M phosphate buffer, 0.15 M NaCl, pH 7.4.

Plain micelles were prepared as reported above using $mPEG_{5\,kDa}$-DSPE.

For biological studies, SD-PEG-DSPE micelles were prepared as reported above using 1% fluorescein-DOPE/SD-PEG-DSPE molar ratio. The dry thin layer was rehydrated with RPMI-1640 at a final 1 mg/mL SD-PEG-DSPE concentration.

Determination of micellar hydrodynamic diameter and size distribution

Micelles size and size distribution were measured by dynamic light scattering analysis. Micelles at a concentration of 2 mg/mL in 0.02 M phosphate buffer, 0.15 M NaCl were used at pH 7.4, and the sample solutions were also adjusted to pH 6.5 and 6.2 by 1 M HCl addition. The micelles were filtered with a 0.45 μm cut-off membrane and analyzed using a Zetasizer Nano S instrument (Malvern Instruments, Malvern, UK) by detecting the backscatter of the beam at an angle of 173°.

Critical micelle concentration

Critical micelle concentration (CMC) was estimated according to the method reported in the literature (Kwon et al., 1993). Briefly, aliquots of 50 μL of a 10 mg/mL pyrene solution in methanol were spiked in tubes and the organic solvent was removed under vacuum. The tubes were added of different volumes of 2 mg/mL of a SD-PEG-DSPE solution in 20 mM phosphate buffer, 0.15 M NaCl at 7.4, and buffer was added to yield 1 mL final volume in order to have final concentrations of unimers ranging from 0 mg/mL to 2 mg/mL. The tubes were shacked at 37°C overnight and then centrifuged at 10,000 rpm for 5 min. The solution was analyzed by fluorescence (λ_{ex} 339 nm; λ_{em} 390 nm). The CMC value was referred to the concentration of the unimer at which a sharp increase in fluorescence was observed. For comparison, the CMC of commercial $mPEG_{5\,kDa}$-DSPE was investigated.

Paclitaxel-loaded micelle preparation

SD-PEG-DSPE (20.4 mg) was dissolved in 3 mL of chloroform and the organic solution was added of 1 mL of methanol containing 2.6 mg of paclitaxel. The solvents were removed by rotary evaporation and the resulting thin layer was rehydrated in 20 mM phosphate buffer, 0.15 M NaCl, pH 7.4 to a final SD-PEG-DSPE concentration of 5 mg/mL. The colloidal dispersion was filtered through a 0.22 μm pore size membrane and the paclitaxel content in the solution was determined by RP-HPLC using a Phenomenex Luna C_{18} column isocratically eluted with acetonitrile/H_2O 55/45 vol/vol containing 0.05% TFA. The UV detector was set at 227 nm and the peak area was referred to a standard curve.

Paclitaxel release studies

4 mL Paclitaxel-loaded micelles in 20 mM phosphate buffer, 0.15 M NaCl pH 7.4 (SD-PEG-DSPE 5 mg/mL) were split in 2 mL samples. One of the samples was adjusted to pH 6.2 by 1 M HCl addition. The two samples were placed into a Spectra/Por regenerated cellulose 3.6 kDa cut-off dialysis membrane (Spectrum Laboratories Inc., Rancho Dominguez, CA) and dialyzed against 45 mL of 20 mM phosphate 0.15 M NaCl at the same pH and at 37°C. At scheduled intervals the receiving buffer volume was replaced with fresh buffer. Paclitaxel was extracted from the removed volume with 5 mL of dichloromethane for four times. The organic solvent was removed under vacuum and the residue redissolved in 300 μL of methanol and analyzed by RP-HPLC as reported above for paclitaxel estimation. The extraction efficiency of the method was validated to be 97.4%

Micelle biocompatibility

MCF7 cells were seeded in a 96-well plates (5000 cells/well) and grown for 24 h in complete RPMI-1640 medium. Afterwards, the medium was replaced with RPMI-1640 at pH 6.2 and 7.4 containing increasing concentrations of either SD-PEG-DSPE or mPEG-DSPE and the cells were incubated at 37°C for 48 h. Each well was added of 20 μL of 5 mg/mL MTT in 20 mM phosphate buffer, 0.15 M NaCl, pH 7.4, and the plates were incubated for further 4 h at 37°C. The medium was then carefully discharged from each well and replaced with 200 μL of DMSO. The plates were gently shaken overnight in order to dissolve the formazan crystals and absorbance was measured by a Bio-Tek Instruments microplate reader (Highland, VT) at 570 nm and at 620 nm as reference. The cell viability was expressed as percentage of the 570 nm/620 nm absorbance ratio (Hansen et al., 1989).

Cell uptake study by fluorimetric analysis of lysates

MCF7 cells were seeded in 6-well tissue culture plates (1.5×10^6 cells/well) and grown for 24 h in complete RPMI-1640 medium. The cells were washed with RPMI-1640 and 2 mL of 1% fluorescein-DOPE-labeled SD-PEG-DSPE or mPEG-DSPE micelles in 20 mM phosphate buffer, 0.15 M NaCl at pH 7.4 or pH 6.2 (1 mg/mL) was added. The plates were incubated at 37°C. At scheduled intervals, the medium was removed, the samples were washed three times with 20 mM phosphate buffer, 0.15 M NaCl at the same pH and detached by ice contact treatment and pipetting (Salmaso et al., 2009). The cells were recovered by centrifugation, lysed by addition of 1 mL of 0.1% triton in water and the lysates were analyzed by fluorescence spectroscopy (λ_{ex} 494 nm, λ_{em} 520 nm). The relative fluorescence was normalized to the cell content that was calculated according to the protein concentration of lysated cells by BCA analysis (Pierce Biotechnology, Inc., Rockford, IL).

Cytofluorimetric analysis

MCF7 cells were seeded in a 12-well plate at a concentration of 5×10^5 cells/well and grown for 48 h. The medium was discharged and the cells were incubated with 0.5 mL/well of medium at pH 7.4 or

Journal of Drug Targeting Downloaded from informahealthcare.com by Radboud Universiteit Nijmegen on 11/04/14
For personal use only.

RIGHTSLINK

6.2 containing 1 mg/mL of 1% fluorescein-DOPE-labeled SD-PEG-DSPE or mPEG-DSPE micelles. The plates were incubated for 4 h at 37°C and then the medium was removed, the cells washed twice with 20 mM phosphate buffer, 0.15 M NaCl at the same pH of incubation and detached by ice cold contact treatment and pipetting. The cells were collected by centrifugation at 1000 rpm for 5 min and resuspended in 1% paraformaldehyde in 20 mM phosphate buffer, 0.15 M NaCl, pH 7.4. The samples were analyzed by cytofluorimetry with a FACSCalibur Flow Cytometer (Becton Dickinson, San Jose, CA). The experiment was performed in triplicate.

Confocal microscopy

After the initial passage in tissue culture flasks, MCF7 cells were seeded in 4-well tissue culture detachable BD-Falcon CultureSlides chambers at a concentration of 2×10^5 cells per well and grown in RPMI-1640 with 10% FBS. After 24 h the chambers were washed twice with RPMI and then incubated at 37°C with 0.5 mL of 1 mg/mL 1% fluorescein-DOPE-labeled SD-PEG-DSPE or mPEG-DSPE micelles in RPMI at pH 7.4 or 6.2. After 2 h, the medium was removed, the samples were washed three times with 20 mM phosphate buffer, 0.15 M NaCl at the same pH of incubation and the cells were fixed by 15 min contact with 0.5 mL of 1% paraformaldehyde in 20 mM phosphate buffer, 0.15 M NaCl, pH 7.4. Individual coverslips were mounted with glass slides using Vectashield mounting medium with DAPI for nuclei staining (Vector Laboratories, Burlingame, CA). The cells were analyzed by confocal scanning laser microscope Leica TCS SP5 (Leica Microsystems CMS, Mannheim, Germany) equipped with a Leica HCX PL APO 63X/1.40 oil immersion objective. The blue fluorescence for DAPI was detected with 351 nm laser illumination and green fluorescence for fluorescein-DOPE with 488 nm laser illumination.

In vitro selective drug delivery

MCF7 cells were seeded at a concentration of 5×10^3 cells/well on a 96-well plate in RPMI-1640 supplemented with 10% FBS and grown for 24 h. Afterwards, the medium was replaced with medium containing 1 mg/mL of 0–50 nM paclitaxel-loaded SD-PEG-DSPE or mPEG-DSPE micelles at pH 7.4 or 6.2. The cells were incubated for 12 h and then the medium was replaced with fresh complete medium and the cells were grown for further 48 h. Cell viability was assessed by the MTT test as reported above.

Results

Synthesis and chemical characterization of SD-PEG-DSPE

The preparation of SD-PEG-DSPE was carried out according to a two-step procedure: (1) synthesis of SD-succ-$CONH(CH_2)_2NH_2$ (SD-succ-ethyl-NH_2); (2) conjugation of SD-succ-ethyl-NH_2 to commercially available NHS-$PEG_{3.4\ kDa}$-DSPE.

Scheme 1 describes the synthesis of SD-succ-ethyl-NH_2. This product was obtained by the SD aniline group amidation by reaction with succinic anhydride, carboxyl group activation to methyl ester and finally reaction with an excess of 1,2-diaminoethane that allowed for the introduction of an amino group in the SD structure. RP-HPLC, ^{1}H NMR, and ESI-TOF analysis demonstrated that the SD succinylation was quantitative yielding a high purity acid intermediate. Also, the subsequent esterification with methanol was found to be a very efficient reaction. Unreacted acetyl chloride was quenched by $NaHCO_3$. The molecule amination was finally carried out by treatment of the methyl ester activated derivative with 20-fold molar excess of 1,2-diaminoethane. Such an excess was necessary in order to avoid unwanted cross-linking reactions. Acetic acid was added to the reaction mixture in order to preserve the SD-succ integrity as it can easily undergo hydrolysis (data not shown). As diethyl ether extraction did not allow for complete elimination of unreacted 1,2-diaminoethane, an additional purification step was efficiently carried out by solid phase extraction. The identity of SD-succ-ethyl-NH_2 and its purity degree were confirmed by chromatographic and spectrometric analysis. ^{1}H NMR and ESI-TOF spectra confirmed the product chemical identity. RP-HPLC chromatogram and the ESI-TOF spectra showed that the reaction yielded a product with high purity degree.

Scheme 2 describes the synthesis of SD-PEG-DSPE that was carried out by reaction of commercial available NHS-$PEG_{3.4\ kDa}$-DSPE with a 20-fold molar excess of SD-succ-NH_2. Large amount of SD-succ-ethyl-NH_2 was used to maximize the product yield. The crude product precipitation in diethyl ether and rehydratation in water

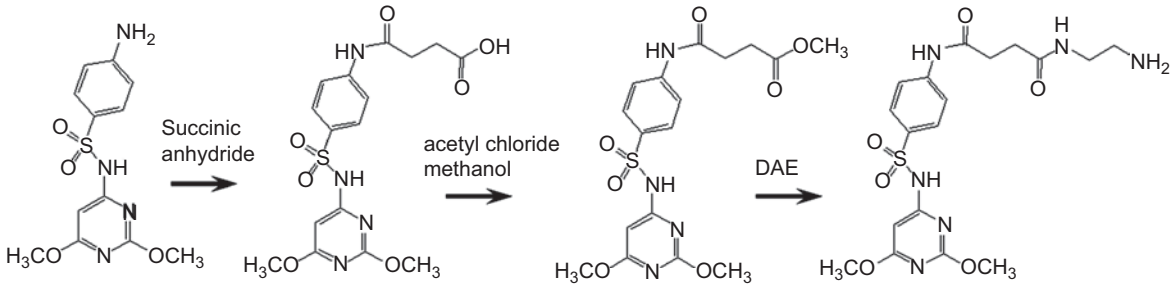

Scheme 1. Synthesis of SD-succ-ethyl-NH_2.

Journal of Drug Targeting Downloaded from informahealthcare.com by Radboud Universiteit Nijmegen on 11/04/14
For personal use only.

© 2011 Informa UK, Ltd.

RIGHTSLINK

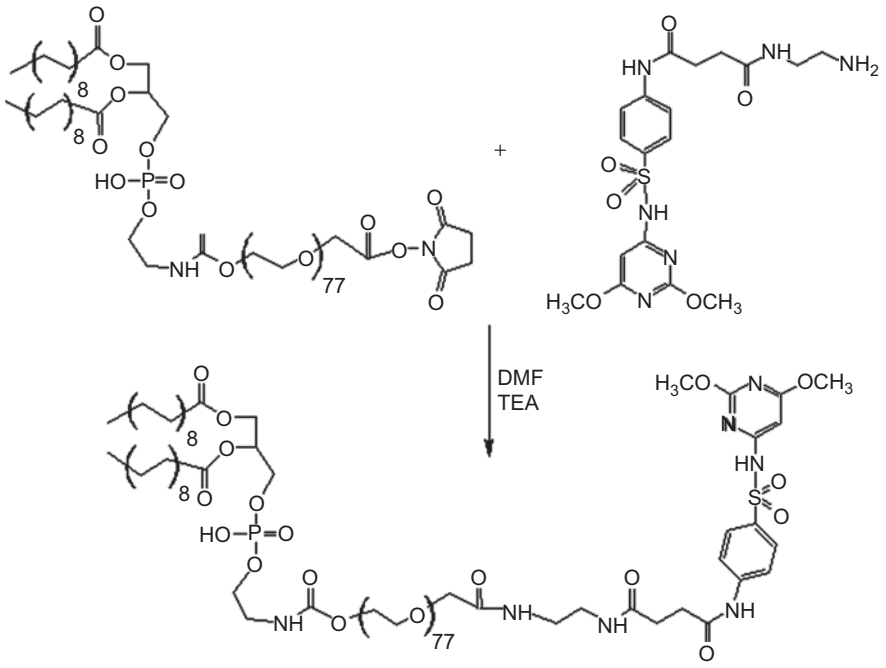

Scheme 2. Synthesis of SD-PEG-DSPE.

allowed for micelle assembling and their fractionation by size exclusion chromatography. Gel chromatography was carried out under slightly basic conditions (pH 8.0) that avoided the possible micelle association into macroaggregates. The RP-HPLC analysis showed that the purification process allowed for complete elimination of the low molecular weight unconjugated SD-succ-ethyl-NH_2. The chemical identity of the purified conjugate was confirmed by ^{1}H NMR spectroscopy. Furthermore, the ^{1}H NMR analysis showed that the reaction yielded 77% NHS-PEG-DSPE conjugation with SD, which is in good agreement with the results obtained by UV-Vis analysis. The NHS-PEG-DSPE derivatization was very high in consideration that the starting material was 91% NHS-activated PEG-DSPE (provider information). According to the analytical results the final product contained 23% of inactivated PEG-DSPE (PEG-DSPE/SD-PEG-DSPE molar percentage).

Physicochemical characterization of SD-PEG-DSPE

Potentiometric analysis was undertaken to investigate acid/base properties of the new SD derivatized phospholipid (Öhman & Sjöberg, 1996). Figure 1 reports the potentiometric profile. The bioconjugate was found to possess a pK_a of 6.7 ± 0.1, which is fairly close to the value reported in literature for SD (Kang & Bae, 2002).

Physical characterization of micelles

The dynamic light scattering profile reported in Figure 2 shows that SD-PEG-DSPE assembles into micelles with ~20 nm mean diameter and narrow size distribution (PDI 0.35–0.619). Micelle size was in fair agreement with data reported in the literature for micelles composed of PEG-phospholipid with similar PEG molecular weight.

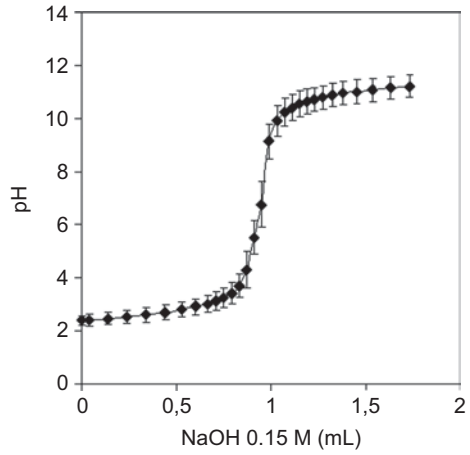

Figure 1. Potentiometric titration of SD-PEG-DSPE dissolved in HCl solution.

The data summarized in Table 1 show that neither the micelle size nor the size distribution were affected by the pH of the colloidal dispersion.

The CMC was found to be 60 μM, which is slightly higher as compared to the values reported in the literature for PEG-phospholipid with similar molecular weight (Lukyanov et al., 2002).

SD-PEG-DSPE biocompatibility

Biocompatibility studies were carried out by MCF7 cell incubation with a wide range of SD-PEG-DSPE concentrations in order to examine the biological effect of the phospholipids derivative either below or above its CMC value. Furthermore, the study was performed at pH 7.4 and 6.2 to evaluate the material impact under different physiopathological conditions. As control, mPEG-

Journal of Drug Targeting Downloaded from informahealthcare.com by Radboud Universiteit Nijmegen on 11/04/14
For personal use only.

RIGHTSLINK

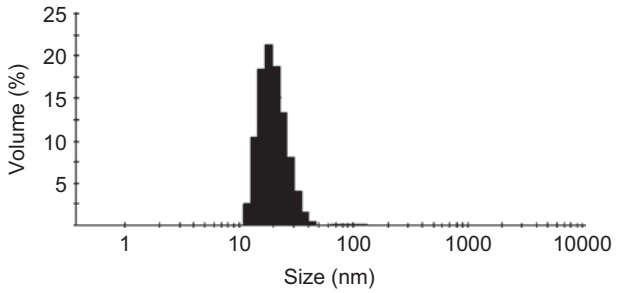

Figure 2. SD-PEG-DSPE-based micelle size analysis in 0.02 M phosphate buffer, 0.15 M NaCl, pH 7.4.

Table 1. Micelle size (mean diameter ± SD, nm) at pH 7.4, 6.5 and 6.2.

pH conditions	Size (nm)
7.4	19.96 ± 11.80
6.5	19.93 ± 13.66
6.2	19.05 ± 14.98

DSPE biocompatibility was investigated under the same experimental conditions.

The cell viability profiles described in Figure 3 show that neither SD-PEG-DSPE (panel A) nor mPEG-DSPE (panel B) elicited cytotoxicity, regardless the unimer concentration or the incubation pH.

Cell uptake studies

The association of micelle/cell at pH 7.4 and 6.2 was investigated by MCF7 cell incubation with fluorescein-labeled SD-PEG-DSPE. Fluorescein-labeled mPEG-DSPE was used as control. The fluorescence values obtained from MCF7 cells lysates are depicted in Figure 4.

The results reported in Figure 4A and B show that the fluorescein-labeled mPEG-DSPE micelles were only slightly taken up by the cells either at pH 7.4 or 6.2. Also the cell uptake of fluorescein-labeled SD-PEG-DSPE micelles was negligible when incubation was carried out at pH 7.4. On the contrary, at pH 6.2, fluorescein-labeled SD-PEG-DSPE-based micelles were significantly taken up by the cells according to a time-dependent behavior. The steady cell uptake was reached in about 5 h. At this time point the cell-associated fluorescence obtained with the SD-PEG-DSPE derivative was 4.8 times higher as compared to that obtained with mPEG-DSPE.

Flow cytometry studies (FACS) partially confirmed the data obtained by fluorescence analysis. The dot plot profiles reported in Figure 5 show that 97.8% and 97.3% of MCF7 cells incubated with mPEG-DSPE micelles at pH 7.4 and 6.2, respectively, have a mean fluorescence intensity (MFI) lower than 70 (19.3 at pH 7.4 and 9.5 at pH 6.2). In the case of SD-PEG-DSPE micelles at pH 7.4, 97.9% of cells had an MFI of 34.0 while after incubation at pH 6.2, 94.0% of cells displayed an MFI of 32. Despite these results indicate that the number of cells involved in the SD-PEG-DSPE micelles uptake at pH 6.2 was only slightly higher (6%) than that incubated with mPEG-DSPE (2.2 and 2.7 at pH 7.4 and 6.2, respectively) and SD-PEG-DSPE micelles at pH 7.4 (2.1%), the MFI (178) of the former was significantly high.

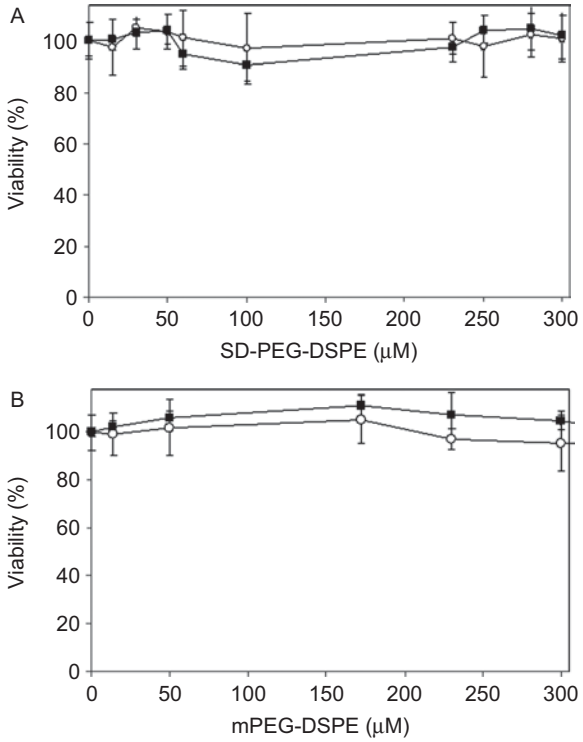

Figure 3. SD-PEG-DSPE (A) and mPEG-DSPE (B) intrinsic cytotoxicity at pH 6.2 (○) and pH 7.4 (▪) after 48 h contact time.

The confocal analysis performed with MCF7 cells incubated with fluorescently labeled micelles at two pH conditions, 7.4 and 6.2, confirmed the results obtained by flow cytometry. The images reported in Figure 6 show that diffused feeble cell fluorescence was obtained at both incubation pH. Nevertheless, at pH 6.2 few cells displayed high fluorescence (Figure 6, panel A). Interestingly, the fluorescein-labeled mPEG-DSPE micelles used as control displayed undetectable fluorescence at both pHs and no cell subpopulation was observed.

Paclitaxel loading and release study

The preparation of paclitaxel-loaded SD-PEG-DSPE micelles resulted in 2.5% drug incorporation (paclitaxel/SD-PEG-DSPE, w/w), which is similar to the payload obtained with mPEG-DSPE micelles reported in the literature (Gao et al., 2002, 2003). The drug release from the micelles was investigated at pH 7.4 and 6.2, which mimic the blood and the tumor interstitial compartment microenvironment, respectively. In order to guarantee sink conditions throughout the study, the releasing buffer was frequently replaced with fresh medium.

The profiles depicted in Figure 7 show that paclitaxel is released from the micelles with similar behavior at pH 7.4 and 6.2. About 5% of the loaded drug was released in 12 h and about 50% in 200 h. Preliminary studies demonstrated that paclitaxel in a micelle-free solution freely diffused through the dialysis membrane as 100% of the incubated drug was dialyzed in 10 h. Therefore,

Journal of Drug Targeting Downloaded from informahealthcare.com by Radboud Universiteit Nijmegen on 11/04/14
For personal use only.

© 2011 Informa UK, Ltd.

RIGHTSLINK

the slow paclitaxel appearance in the releasing medium could not be attributed to drug/dialysis membrane interaction phenomena.

Cell culture studies carried out by MCF7 cell incubation with paclitaxel-loaded SD-PEG-DSPE micelles at pH 6.2 and 7.4 were undertaken to evaluate the effect of the SD decoration on the drug delivery properties of the colloidal formulation. The cell culture protocol was adapted to emphasize the pH-sensitive micelle contribution to the drug uptake. As compared to other protocols reported in the literature, a short exposition to drug-loaded carrier could provide for a better discrimination between the two pH conditions (Michalakis et al., 2005; Nonaka et al., 2006). As a control, studies were performed under the same conditions using paclitaxel-loaded mPEG-DSPE micelles. The results reported in Figure 8 show that the former have higher toxic effect than the latter. These results are in fair agreement with the higher cell interaction properties of SD-PEG-DSPE micelles as compared to the mPEG-DSPE formulations. However, though the fluorescence studies showed that the SD-PEG-DSPE micelles are taken up by cells according to a pH-dependent mechanism, the cytotoxicity studies showed only slight differences in the drug delivery performance between pH 7.4 and 6.2. At acidic condition, paclitaxel-loaded SD-PEG-DSPE micelles have EC_{50} of 2 nM which is very close to the values obtained with paclitaxel in solution, while at pH 7.4 the EC_{50} value was 5 nM (Figure 8, panel A). Control micelles displayed higher EC_{50} values: 10 and 15 nM at pH 7.4 and 6.2, respectively (Figure 8, panel B).

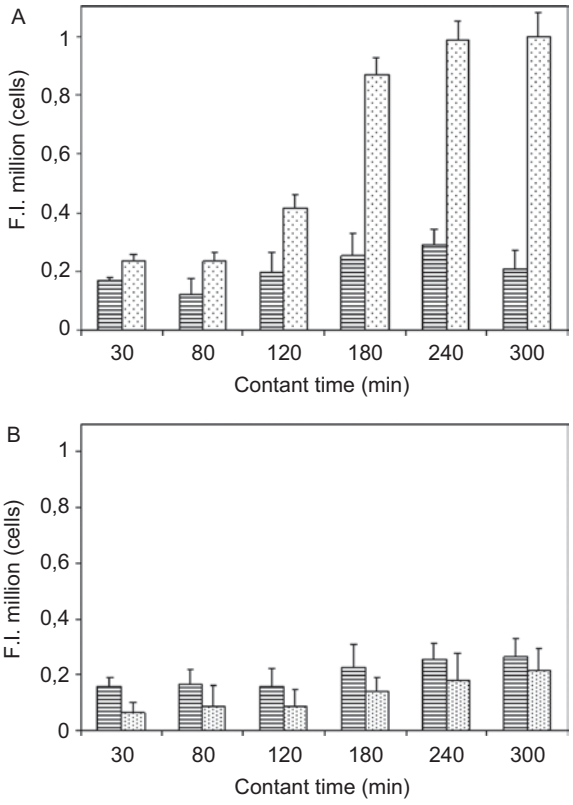

Figure 4. Time course fluorescence profiles of lysated MCF7 cells after cell incubation with fluorescein-DOPE-labeled SD-PEG-DSPE (A) and mPEG-DSPE (B) micelles. The cells were incubated at pH 6.2 (dotted columns) and 7.4 (dashed columns).

Discussion

Poly(ethylene glycol) phospholipids were conjugated with SD to obtain pH-sensitive amphiphilic derivatives (SD-PEG-DSPE) that can reversibly switch from the ionized to the deionized form in a narrow pH range. According to the SD pK_a, the phospholipids derivatives may undergo hydrophilic/hydrophobic changes within the physiopathological microenvironmental conditions. Therefore, SD-PEG-DSPE micelles can be triggered into the tumor site, where the environment is mildly acidic as compared to blood, providing for site selective drug delivery (Vaupel et al., 1989).

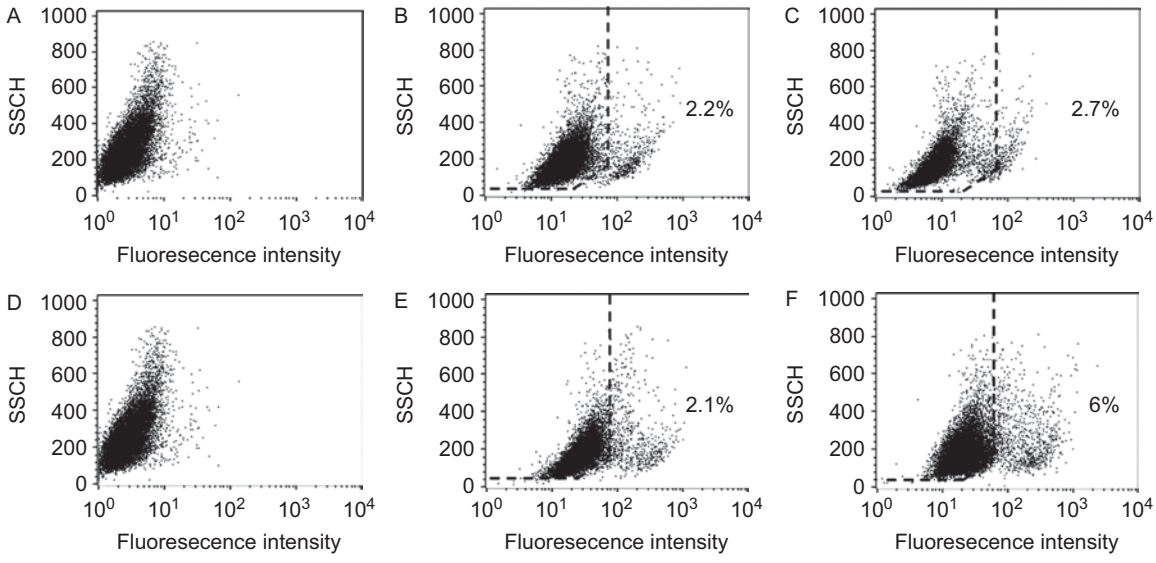

Figure 5. FACS analysis of MCF7 cells incubated without carrier at pH 7.4 and 6.2 (panels A and D, respectively). Cells were treated with fluorescein-labeled mPEG-DSPE (panel B and C) and SD-PEG-PE micelles (panel E and F) at pH 7.4 (panel B and E) and 6.2 (panel C and F).

Journal of Drug Targeting Downloaded from informahealthcare.com by Radboud Universiteit Nijmegen on 11/04/14
For personal use only.

RIGHTSLINK

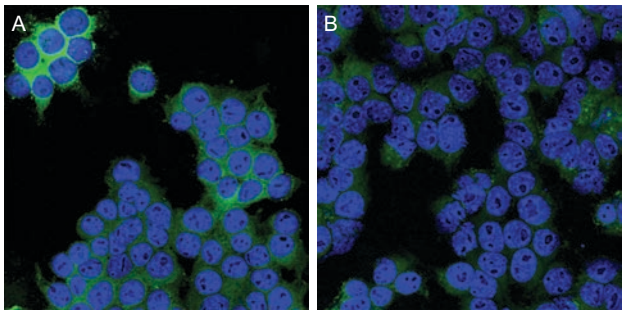

Figure 6. Confocal microscopic examination of MCF7 treated with SD-PEG-DSPE micelles 1% DOPE-fluorescein at pH 6.2 (A) and 7.4 (B). Cell images were acquired in blue channel for nuclei detection after labeling with DAPI and green channel for fluorescein-labeled micelle detection.

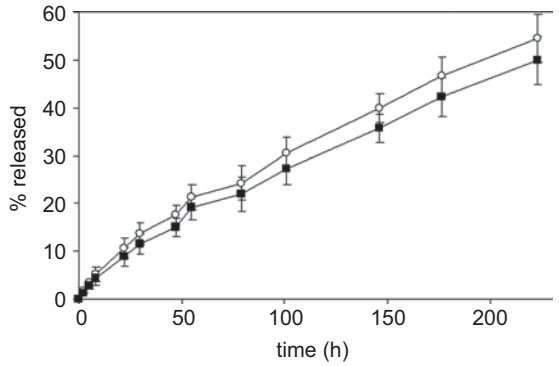

Figure 7. Release kinetic profile of paclitaxel from SD-PEG-DSPE micelles at pH 6.2 (▪) and 7.4 (○).

SD-PEG-DSPE unimers were synthesized according to a simple, reproducible, and efficient protocol, as demonstrated by the spectrometric and chromatographic analysis of intermediates and final product. The use of proper reaction conditions resulted in high product yield and purity degree. In the first step, the bicarbonate addition to the carboxylated SD activation reaction avoided degradation phenomena due to hydrochloric acid released by thionyl chloride, while the use of a large excess of 1,2-diaminoethane for the SD amination prevented the product dimerization. In the second step, excess of SD-succ-ethyl-NH_2 was used to achieve high reaction yield with NHS-PEG-DSPE and then the unreacted reagent was eliminated by gel chromatography.

The potentiometric analysis showed that the SD-PEG-DSPE unimers have pK_a of 6.7, which is slightly higher as compared to SD pK_a reported in the literature. This difference may be ascribed to the presence of hydrated and hindered PEG chains that can alter the SD microenvironment and protonation.

The SD-PEG-DSPE unimers were found to assemble in aqueous medium to produce micelles with ~20 nm diameter, which is the typical size of these nanosystems (Lukyanov et al., 2002). The micelle dimension was not significantly affected by the pH conditions indicating that under the experimental conditions the hydrophobic character of SD at acidic pH does not induce significant

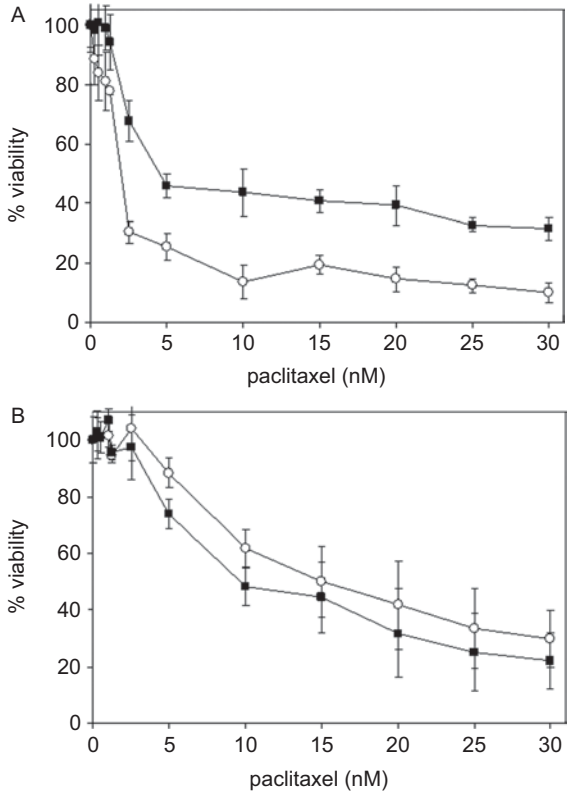

Figure 8. Cytotoxicity profiles obtained by MCF7 cell incubation with paclitaxel-loaded SD-PEG-DSPE (A) and mPEG-DSPE (B) micelles at pH 6.2 (○) and 7.4 (▪).

morphological changes, namely bending of the polymer chains, disassembling of the unimers or micelles aggregation. The CMC value was slightly higher as compared to that obtained with mPEG-DSPE reported in the literature, probably because the presence of the negative charges of SD on the micelle surface promotes PEG chain repulsion. Nevertheless, the CMC was low enough to bestow high thermodynamic stability on micelles, preventing their de-aggregation upon dilution. Micelle stability is a requisite in the development of physically assembled drug delivery systems as the association integrity must be maintained in the bloodstream while structural alterations guarantee site selective drug release (Lukyanov et al., 2002).

Cell culture studies carried out by quantitative analysis of cells incubated with SD-PEG-DSPE fluorescently labeled with fluorescein-DOPE showed that the micelles interact with cells. However, cell toxicity studies showed that the SD-PEG-DSPE interaction did not hamper the cell biological activity either in the unimer or in the micellar form, underlining the high biocompatibility of this material. Cell/SD-PEG-DSPE micelle interaction was found to take place according to a pH-dependent behavior. The amount of a lipid core–loaded fluorescence probe taken up by the cells incubated with SD-PEG-DSPE micelles at pH 6.2 was significantly higher than that obtained at pH 7.4 and with mPEG-DSPE micelles. Furthermore, the time-dependent cell uptake observed at pH 6.2 with the pH-sensitive micelles seems to

Journal of Drug Targeting Downloaded from informahealthcare.com by Radboud Universiteit Nijmegen on 11/04/14
For personal use only.

© 2011 Informa UK, Ltd.

RIGHTSLINK

indicate that the internalization process undergoes cell saturation. These results were in apparent contradiction with the flow cytofluorimetry and confocal microscopy data, which showed that the micelles could be taken up by all cells regardless the incubation pH. Nevertheless, both cytofluorimetry and confocal microscopy analysis clearly indicated that the higher cell uptake of SD-PEG-DSPE micelles at pH 6.2 as compared to SD-PEG-DSPE micelles at pH 7.4 or to mPEG-DSPE micelles could be ascribed to a cell subpopulation, about 6% of the incubated cells, which was significantly active in micelle payload internalization under acidic conditions. This unexpected behavior may be due to specific cell cycle phase associated uptake. Additionally, the confocal images showed that no fluorescence was associated to the nucleus while it was located in the membrane and cytosolic compartment.

The feasibility to use SD-PEG-DSPE micelles for drug delivery was verified with paclitaxel, a poorly soluble and unstable anticancer drug. Paclitaxel was efficiently incorporated into the lipid core of micelles resulting in dramatic solubility increase, from 0.3 μg/mL (Choa et al., 2004) to 125 μg/mL. The slow drug release observed *in vitro* highlights the high stability of paclitaxel-loaded system, which is in agreement with the high micelle stability shown by the CMC value. Actually, the high stability of the micelles at pH 7.4 is pre-requisite to avoid the systemic drug release that may be responsible for unspecific toxicity. On the other hand, the slow drug release observed in buffer at pH 6.2 suggests that micelles are stable under acidic conditions too, but the drug may be released upon tumor cell interaction that is promoted by the lower pH in this tissue. However, it should be noted that, although the drug release has been evaluated in buffer which simulates physiological conditions, a different behavior is expected in blood or the tumor tissue. Therefore additional investigations will be undertaken to examine the micelle behavior either in *ex vivo* matrices or *in vivo*.

The drug delivery performance of the pH-sensitive formulation was investigated by paclitaxel-loaded SD-PEG-DSPE micelles with cells at pH 7.4 and 6.2. The cytotoxicity profiles showed a slight but significant difference in paclitaxel delivery obtained with SD-PEG-DSPE micelles at pH 6.2 as compared to the same formulation at pH 7.4, indicating higher intracellular paclitaxel delivery at pH 6.2. Such a selectivity is also supported by the data obtained with mPEG-DSPE micelles that did not show any differences between the cytotoxicity profiles obtained at the two pHs. These results are once again in good agreement with the physicochemical and biopharmaceutical properties of the pH-sensitive micelles previously discussed. The higher paclitaxel delivery observed at pH 6.2 as compared to that at pH 7.4 highlights the pH-sensitive properties of the colloidal carriers showed with the fluorescence studies. On the other hand, the only limited increase in cell toxicity observed at pH 6.2 may be ascribed to the restricted micelles interaction to a cell subpopulation as observed by flow cytometry and confocal analysis.

Conclusions

The data described in this paper show that pH-sensitive micelles can be obtained by conjugating SD to amphiphilic molecules which spontaneously self assemble into colloidal structures. The resulting materials possess the requisites for pharmaceutical application, namely biocompatibility, high drug payload, and stability in the body compartment. Furthermore, the SD decoration endows micelles that can interact with cells to provide for selective drug delivery into tumor site.

However, although the results show the potential applicability of these formulations for tumor targeting opening interesting perspectives in the development of these systems for chemotherapy, it was shown that the attachment of one SD moiety is not *per se* sufficient to guarantee extensive drug release into the tumor cells.

Declaration of interest

The authors report no conflicts of interest.

References

Choa YW, Leeb J, Leeb SC, Huhb KM, Parkb K. (2004). Hydrotropic agents for study of *in vitro* paclitaxel release from polymeric micelles. J Control Release, 97, 249–257.

De S, Robinson DH. (2004). Particle size and temperature effect on the physical stability of PLGA nanospheres and microspheres containing Bodipy. AAPS PharmSciTech, 5, e53.

Gao Z, Lukyanov AN, Chakilam AR, Torchilin VP. (2003). PEG-PE/phosphatidylcholine mixed immunomicelles specifically deliver encapsulated taxol to tumor cells of different origin and promote their efficient killing. J Drug Target, 11, 87–92.

Gao Z, Lukyanov AN, Singhal A, Torchilin VP. (2002). Diacyllipid-polymer micelles as nanocarriers for poorly soluble anticancer drugs. Nano Lett, 2, 979–982.

Gerweck LE, Seetharaman K. (1996). Cellular pH gradient in tumor versus normal tissue: potential exploitation for the treatment of cancer. Cancer Res, 56, 1194–1198.

Hansen MB, Nielsen SE, Berg K. (1989). Re-examination and further development of a precise and rapid dye method for measuring cell growth/cell kill. J Immunol Methods, 119, 203–210.

Kang SI, Bae YN. (2001). pH-induced volume-phase transition by reversible crystal formation. Macromolecules, 34, 8173–8178.

Kang SI, Bae YH. (2002). pH-induced solubility transition of sulfonamide-based polymers. J Control Release, 80, 145–155.

Kumari A, Yadav SK, Yadav SC. (2010). Biodegradable polymeric nanoparticles based drug delivery systems. Colloids Surf B Biointerfaces, 75, 1–18.

Kwon G, Naito M, Yokoyama M, Okano T, Sakurai Y, Kataoka K. (1993). Micelles based on AB block copolymers of poly(ethylene oxide) and poly(beta-benzyl L-aspartate). Langmuir, 9, 945–949.

Lukyanov AN, Gao Z, Mazzola L, Torchilin VP. (2002). Polyethylene glycol-diacyllipid micelles demonstrate increased acculumation in subcutaneous tumors in mice. Pharm Res, 19, 1424–1429.

Lukyanov AN, Torchilin VP. (2004). Micelles from lipid derivatives of water-soluble polymers as delivery systems for poorly soluble drugs. Adv Drug Deliv Rev, 56, 1273–1289.

Makino K, Kado H, Ohshima H. (2001). Aggregation behavior of poly(N-isopropylacrylamide) microspheres. Colloids Surf B Biointerfaces, 20, 347–353.

Journal of Drug Targeting Downloaded from informahealthcare.com by Radboud Universiteit Nijmegen on 11/04/14
For personal use only.

RIGHTSLINK

Matsumura Y, Maeda H. (1986). A new concept for macromolecular therapeutics in cancer chemotherapy: mechanism of tumoritropic accumulation of proteins and the antitumor agent smancs. Cancer Res, 46, 6387–6392.

Michalakis J, Georgatos SD, Romanos J, Koutala H, Georgoulias V, Tsiftsis D, Theodoropoulos PA. (2005). Micromolar taxol, with or without hyperthermia, induces mitotic catastrophe and cell necrosis in HeLa cells. Cancer Chemother Pharmacol, 56, 615–622.

Na K, Lee ES, Bae YH. (2003). Adriamycin loaded pullulan acetate/sulfonamide conjugate nanoparticles responding to tumor pH: pH-dependent cell interaction, internalization and cytotoxicity *in vitro*. J Control Release, 87, 3–13.

Na K, Lee KH, Bae YH. (2004). pH-sensitivity and pH-dependent interior structural change of self-assembled hydrogel nanoparticles of pullulan acetate/oligo-sulfonamide conjugate. J Control Release, 97, 513–525.

Nonaka M, Ikeda H, Fujisawa A, Uehara M, Inokuchi T. (2006). Induction of apoptosis by paclitaxel in human oral carcinoma cells. Int J Oral Maxillofac Surg, 35, 649–652.

Öhman LO, Sjöberg S. (1996). The experimental determination of thermodynamic properties for aqueous aluminium complex. Coord Chem Rev, 149, 33–57.

Owens DE 3rd, Peppas NA. (2006). Opsonization, biodistribution, and pharmacokinetics of polymeric nanoparticles. Int J Pharm, 307, 93–102.

Panyam J, Labhasetwar V. (2003). Biodegradable nanoparticles for drug and gene delivery to cells and tissue. Adv Drug Deliv Rev, 55, 329–347.

Sadagopa Ramanujam VM, Made Gowda NM, Trieff NM, Legator MS. (1980). Ultraviolet spectrophotometric assay of *p*-aminobenzenesulfonamides. Microchemical J, 25, 295–300.

Salmaso S, Bersani S, Elvassore N, Bertucco A, Caliceti P. (2009). Biopharmaceutical characterisation of insulin and recombinant human growth hormone loaded lipid submicron particles produced by supercritical gas micro-atomisation. Int J Pharm, 379, 51–58.

Salmaso S, Pappalardo JS, Sawant RR, Musacchio T, Rockwell K, Caliceti P, Torchilin VP. (2009). Targeting glioma cells *in vitro* with ascorbate-conjugated pharmaceutical nanocarriers. Bioconjug Chem, 20, 2348–2355.

Sims GE, Snape TJ. (1980). A method for the estimation of polyethylene glycol in plasma protein fractions. Anal Biochem, 107, 60–63.

Stefanadis C, Chrysochoou C, Markou D, Petraki K, Panagiotakos DB, Fasoulakis C, Kyriakidis A, Papadimitriou C, Toutouzas PK. (2001). Increased temperature of malignant urinary bladder tumors *in vivo*: the application of a new method based on a catheter technique. J Clin Oncol, 19, 676–681.

Tannock IF, Rotin D. (1989). Acid pH in tumors and its potential for therapeutic exploitation. Cancer Res, 49, 4373–4384.

Torchilin VP. (2007). Micellar nanocarriers: pharmaceutical perspectives. Pharm Res, 24, 1–16.

Vaupel P, Kallinowski F, Okunieff P. (1989). Blood flow, oxygen and nutrient supply, and metabolic microenvironment of human tumors: a review. Cancer Res, 49, 6449–6465.

Verrecchia T, Spenlehaur G, Brazile DV, Murry-Brelier A, Archimbaud Y, Veillard MV. (1995). Non-stealth (poly(lactic acid/albumin)) and stealth (poly(lactic acid-polyethylene glycol)) nanoparticles as injectable drug carriers. J Control Release, 36, 49–61.

Yokoyama M, Miyauchi M, Yamada N, Okano T, Sakurai Y, Kataoka K, Inoue S. (1990). Characterization and anticancer activity of the micelle-forming polymeric anticancer drug adriamycin-conjugated poly(ethylene glycol)-poly(aspartic acid) block copolymer. Cancer Res, 50, 1693–1700.

Zhang JX, Hansen CB, Allen TM, Boey A, Boch R. (2003). Lipid-derivatized poly(ethylene glycol) micellar formulations of benzoporphyrin derivatives. J Control Release, 86, 323–338.

Journal of Drug Targeting Downloaded from informahealthcare.com by Radboud Universiteit Nijmegen on 11/04/14
For personal use only.

© 2011 Informa UK, Ltd.

RIGHTSLINK